# ADVANCED OPTICAL MATERIALS

## PLASMONICS

When a droplet hits the surface of water, it is often observed that a water column, or 'back-jet', surges upwards. Counterintuitive though it might be, a similar phenomenon can occur when ultrafast light pulses shine on a nanostructured metal surface. These sub-wavelength 'nanojets' occur in the regions of highest local field enhancements. For more details, see the article by V. K. Valev et al. on page OP29.

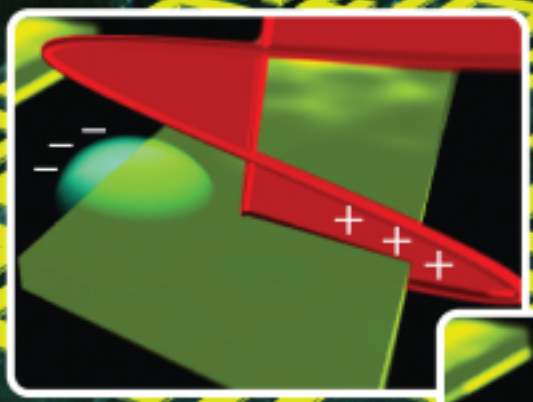

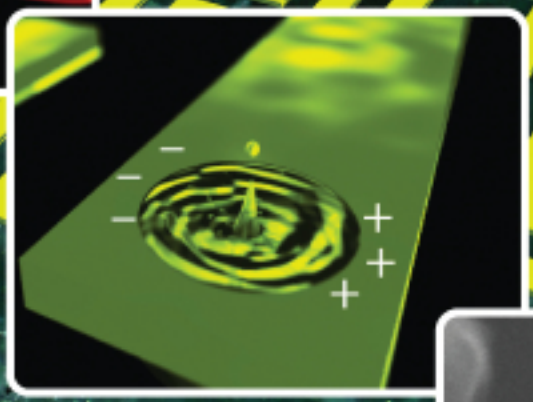

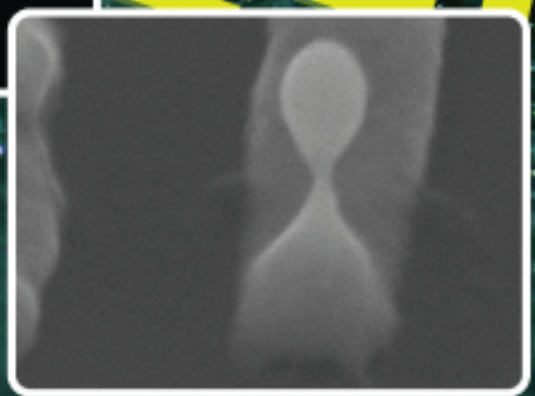

WILEY-VCH

# Plasmon-Enhanced Sub-Wavelength Laser Ablation: Plasmonic Nanojets

*Ventsislav K. Valev,* Denitza Denkova, Xuezhi Zheng, Arseniy I. Kuznetsov, Carsten Reinhardt, Boris N. Chichkov, Gichka Tsutsumanova, Edward J. Osley, Veselin Petkov, Ben De Clercq, Alejandro V. Silhanek, Yogesh Jeyaram, Vladimir Volskiy, Paul A. Warburton, Guy A. E. Vandenbosch, Stoyan Russev, Oleg A. Aktsipetrov, Marcel Ameloot, Victor V. Moshchalkov, and Thierry Verbiest*

When a pebble drops on the surface of water, it is often observed that a water column, or "back-jet", surges upwards. Counter-intuitive though it might be, a similar phenomenon can occur when light shines on a metal film surface. Indeed, tightly focused femtosecond laser pulses carry sufficient energy to locally melt the surface of gold film and the impact from these laser pulses produces a nanojet, as has been theoretically described[1,2] and experimentally demonstrated.[3–5] In particular, these studies show that the very fast cooling rate of the nanojet, allows it to "freeze" in shape, as the temperature drops below the melting point.[6] The gold surface can therefore be imprinted with nanostructures, each marking the point of impact of a laser pulse. Moreover, just as is the case with water, nanojet can result in the projection of a small droplet. Recently, this phenomenon led to the development of a nanofabrication technique, whereby gold spheres with very regular dimensions are collected and assembled into nanopatterns.[7–10] Nanopatterns can also be produced on the gold surface itself with the help of local field enhancements resulting from bringing either a sharp tip[11,12] or spheres close to the surface.[13] But what if the gold surface was nanopatterned to begin with, see **Figure 1**a?

For nanostructures with thickness much smaller than the wavelength of light, because the absorption length of the laser radiation is larger than the thickness of the nanostructure, it was first reported that the temperature stays almost homogeneous over the whole volume of each nanostructure.[14] Consequently, upon illumination and melting of the nanostructures the shape change starts from the sharpest regions, where the forces due to surface tension are high. The reshaping process continues until the nanostructure forms a sphere, minimizing surface tension. At this point the nanostructure constitutes a droplet of melted material and it can be ejected from the surface. This physical mechanism was later refined since it was shown that the temperature over the volume of the nanoparticles can become inhomogeneous.[15] More specifically, it was reported that near curved surfaces, optical near-fields can locally heat up the material and lower the ablation threshold. The mechanism of the ablation was not demonstrated directly.

Dr. V. K. Valev, Prof. T. Verbiest
Molecular Electronics and Photonics
INPAC, Katholieke Universiteit Leuven, BE-3001, Belgium
E-mail: v.k.valev@fys.kuleuven.be
D. Denkova, Y. Jeyaram, Prof. V. V. Moshchalkov
Superconductivity and Magnetism & Pulsed Fields Group
INPAC, Katholieke Universiteit Leuven, BE-3001, Belgium
Prof. A. V. Silhanek
Département de Physique
Université de Liège
Bât. B5, Allée du 6 août, 17, Sart Tilman, B-4000, Belgium
B. De Clercq, Prof. M. Ameloot
University Hasselt and transnational University Limburg
BIOMED, Diepenbeek, Belgium
Prof. O. A. Aktsipetrov
Department of Physics
Moscow State University
11992 Moscow, Russia
Dr. V. Petkov
Dept. Metallurgy and Materials Engineering
Katholieke Universiteit Leuven
Kasteelpark Arenberg 44, B-3001, Belgium
X. Zheng, Dr. V. Volskiy, Prof. G. A. E. Vandenbosch
SAT-TELEMIC, Katholieke Universiteit Leuven
B-3001 Leuven, Belgium
Dr. C. Reinhardt, Prof. B. N. Chichkov
Laser Zentrum Hannover e.V., D-30419 Hanover, Germany
Dr. A. I. Kuznetsov
Advanced Concepts Group
Data Storage Institute 5
Engineering Drive I, 117608, Singapore
Dr. G. Tsutsumanova, Prof. S. Russev
Department of Solid State Physics
Faculty of Physics
Sofia University
Sofia 1164, Bulgaria
E. J. Osley, Dr. P. A. Warburton
London Centre for Nanotechnology
University College London
17-19 Gordon Street, London, WC1H 0AH, United Kingdom
Department of Electronic and Electrical Engineering
University College London
Torrington Place, London, WC1E 7JE, United Kingdom

**DOI: 10.1002/adma.201103807**

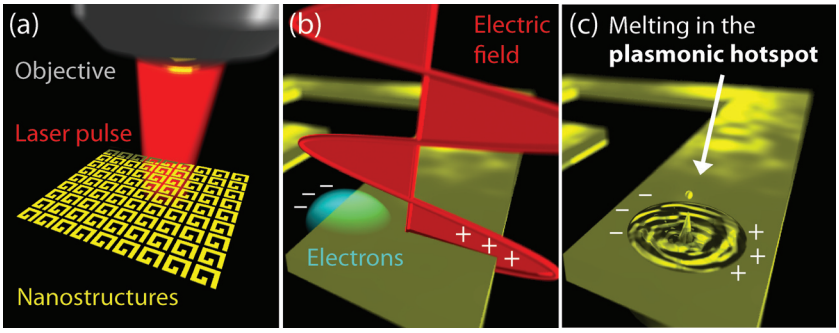


**Figure 1.** In (a), schematic (not to scale) representation of the experiment. In (b), in response to the incident light's electric field, the electron density oscillates in the plasmonic hotspots. These electron oscillations constitute an electric current. Associated Ohmic losses raise the temperature of the material within the plasmonic hotspot above that of the rest of the nanostructure. In (c), due to laser energy deposition by the femtosecond pulses, the temperature within the hotspot is additionally increased above the melting point. A nanojet can then be observed precisely in the plasmonic hotspots, while for the rest of the nanostructure the temperature remains below the melting point and therefore there are no nanojets.

The authors also suggested, but did not show, that a similar local heating could be achieved by means of optical near-fields that are plasmon-enhanced.

Surface plasmon resonances are coherent electron oscillations at the interface between air and metal[16] These plasmons can be excited very efficiently with light, see Figure 1b. Furthermore, depending on the particular geometry of the nanopatterned metal, the plasmons are usually very inhomogeneously distributed on the surface of the nanostructures and can form "hotspots". Plasmons are interesting because they can greatly enhance the local fields. Moreover, unlike sharp geometries, which remain sharp regardless of the illumination wavelength, plasmons are wavelength specific. This can be very advantageous because a nanostructure can support different plasmon modes depending on wavelength, i.e. the location of hotspots can be tuned with the wavelength of light. Moreover, plasmon modes are polarization-specific, which offers additional tunability. To summarize, plasmonic hotspots are regions on the nanostructures where the amplitude of electron oscillations, that are due to light, is maximal. Because electron oscillations constitute an electric current and because electric currents heat up the material by means of Ohmic losses, it follows that the hotspots are literally hot. Consequently, nanopatterning a metal surface leads to *strongly inhomogeneous heating* upon illumination, which has immediate consequences for the melting process.

If laser heating of the metal surface is inhomogeneous, then the laser intensity can be tuned so that melting occurs in the hotspots but not throughout the rest of the structure, see Figure 1c. As the laser irradiates such a surface, nanojets and the associated nanobumps can mark the hotspots. In fact, such nanobumps were already observed in the precise locations of plasmonic hotspots on a *nickel* surface,[17] although the nanobumps' origin was not clearly identified. Nevertheless, it was recognized that the nanobumps can constitute an efficient method for visualizing plasmonic hotspots. It was also reported that no nanobumps had been observed on a gold surface – a rather severe limitation since gold is the material of choice for plasmonic nanotechnology. Here, we propose a very clear and straightforward physical mechanism for the occurrence of nanobumps and demonstrate their presence on a *gold* surface. This insight into the basic interactions of light and materials at the nanoscale opens up new possibilities for applications. The latter can include, for instance, laser-induced transfer fabrication of nanospheres, whose radius is determined by the plasmonic properties of a nanopatterned gold surface.[7–10] Another example is electronic chips where the interconnects between transistors could be ensured by laser-induced, and plasmon-assisted, metal melting.

Because it has been established that we can change the location of the hotspots by changing the incident polarization in G-shaped nanostructures made of both gold[18–20] and nickel,[21] we begin by choosing a G-shaped design, see **Figure 2**a, where both gold and nickel are deposited, see Figure 2b. More details on the deposition and on the rest of the sample preparation can be found in Ref. [22]. After preparation, electron energy-dispersive x-ray spectroscopy (EDS) reveals that the nanostructures (in Figure 2c) contain, indeed, both gold (Figure 2d) and nickel (Figure 2e). The quality of the sample preparation is checked with scanning electron microscopy (SEM) and with atomic force microscopy (AFM), see **Figure 3**a. This figure shows that the nanostructures' surfaces are rather smooth… before illumination.

First, illumination of the nanostructures is performed with Ti:Sapphire laser pulses, of approximately 120 fs duration, at a wavelength of 800 nm. The laser light is focused with a ×100 objective, NA = 1.46, to a spot of 330 nm by 440 nm, with an average power of 0.82 mW and pixel dwell time of 0.571 µs. The samples are illuminated with light polarized linearly along both the horizontal and vertical directions. These directions are indicated with a red and a green arrow, respectively, in Figure 3. Figure 3b and Figure 3d show AFM micrographs of the nanostructures following illumination with horizontally and vertically polarized light respectively. In contrast to Figure 3a, regular patterns of nanobumps at the surface of the sample can now be seen. For clarity, these white spots have been encircled in red and green, depending on the polarization direction of light. The precise location of these nanobumps depends on the direction of linearly polarized light. For horizontally polarized light, the nanobumps are situated along horizontal edges of the nanostructures, whereas for vertically polarized light they are situated along the vertical edges. Since both gold and nickel are present in the nanostructures, it is important to understand what material are these nanobumps made of.

Energy-dispersive x-ray spectroscopy (EDS) is an element specific technique which can be used to evaluate the relative increase or decrease of material at the nanobumps. In order to ensure the reproducibility of our results, EDS was performed with two different instruments, in two separate research groups. Figure 3d and Figure 3e show data obtained from EDS scans along the nanostructures and through the nanobumps. The exact path of the scans is indicated with a green line in

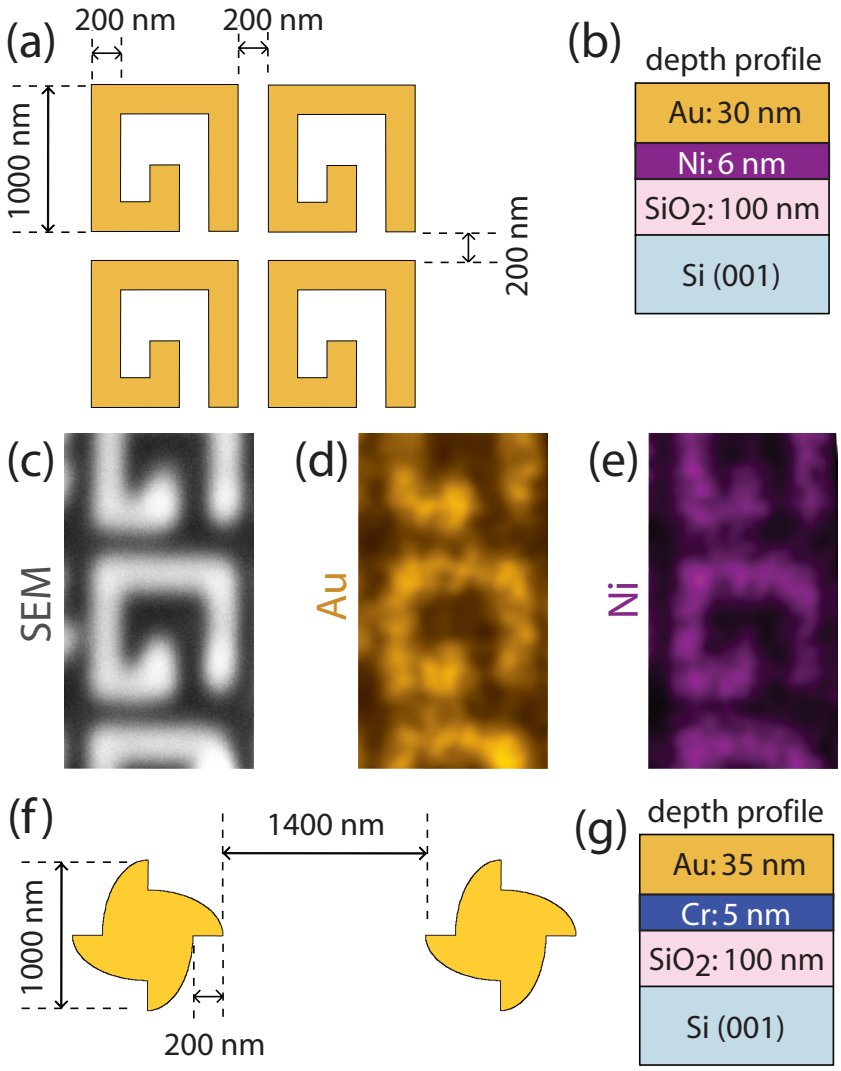


**Figure 2.** The plasmonic nanostructures within the sample arrays are made of gold, on top of Ni or Cr adhesion layer. For the G-shaped nanostructures, the nominal size and depth profile of the sample are shown in (a) and (b) respectively. Scanning electron microscopy of the actual structures is presented in (c), and energy-dispersive x-ray spectroscopy demonstrates that continuous layers of both gold, in (d), and nickel, in (e), are present. For the star-shaped nanostructures, the nominal size and depth profile are shown in (f) and (g) respectively.

the insets. More specifically, Figure 3d demonstrates that, in the nanobump, there is a clear increase of the signal from gold, with respect to the rest of the nanostructure. Simultaneously, nickel signal remains constant throughout the entire nanostructure. The data indicate that this particular nanobump is made of gold; others however are not. Indeed, in Figure 3e, the EDS scan crosses four nanobumps. Based on the observation of increased EDS signal, the first two nanobumps appear to contain both gold and nickel, while the third contains mostly nickel and the fourth mostly gold. This seemingly random material content suggests that the nanobumps are made of a gold/nickel melt. Furthermore, the presence of a metal melt provides a straightforward explanation of the nanostructures as nanojet formation, associated with the femtosecond laser pulses. Obviously, the melting process is caused by light but what evidence is there for the exact cause involved; why is there a regular pattern of melted material rather than a homogeneous melting on the edges of the entire nanostructure?

Numerical simulations constitute a very informative tool for studying the interactions of light with plasmonic nanostructures. We have performed numerical simulations with the MAGMAS Maxwell equations solver.[23] **Figure 4**a and Figure 4b present simulations of the charge distribution at the surface of our nanostructures, under the influence of horizontally and vertically linearly polarized light, respectively. It can be seen that in each case, the direction of polarization determines the direction of charge separation and that the charges accumulate on the edges of the nanostructures. Moreover, the sign of the charges represented in Figure 4a and Figure 4b oscillates at the frequency of light. Consequently, between the regions of positive and negative charge, electric currents flow. According to Joule's law, these electric currents heat up the material; the heating being proportional to the square of the electric currents. Their precise location is strongly dependent on the geometry of the nanostructure. Figure 4c and Figure 4d show the distribution of the squared electric currents corresponding to the charge distributions in Figure 4a and Figure 4b, respectively. For comparison, the pattern of the nanobumps has been reproduced by means of colored circles and superimposed on the simulation results. The figures demonstrate that there is an unambiguous match between the regions where nanobumps and high electric currents occur. Naturally, the simulated structures have an ideal geometry, while the measured ones present numerous fabrication imperfections; therefore the match cannot be expected to be absolutely exact. Nevertheless, the largest nanobumps, situated at both ends of the nanospiral in Figure 3b, clearly correspond to the regions of highest local currents, in Figure 4c. Because electric currents heat up the material through Ohmic losses, the regions of high electric currents constitute, literally, hotspots on the sample surface. Therefore, as we increase incoming laser power, melting of the sample takes place in the hotspots, before the rest of the nanostructures. This process could be unambiguously demonstrated upon increasing the laser power and observing progressive melting originating in the hotspots. Here we begin by showing that the processes at study are not specific to the G-shaped sample geometry and turn our attention to star-shaped nanostructures.

In the star-shaped nanostructures, numerical simulations demonstrate that the structures exhibit localized plasmons depending on polarization. **Figure 5**a and Figure 5b shows that for horizontal polarization, two plasmonic hotspots should

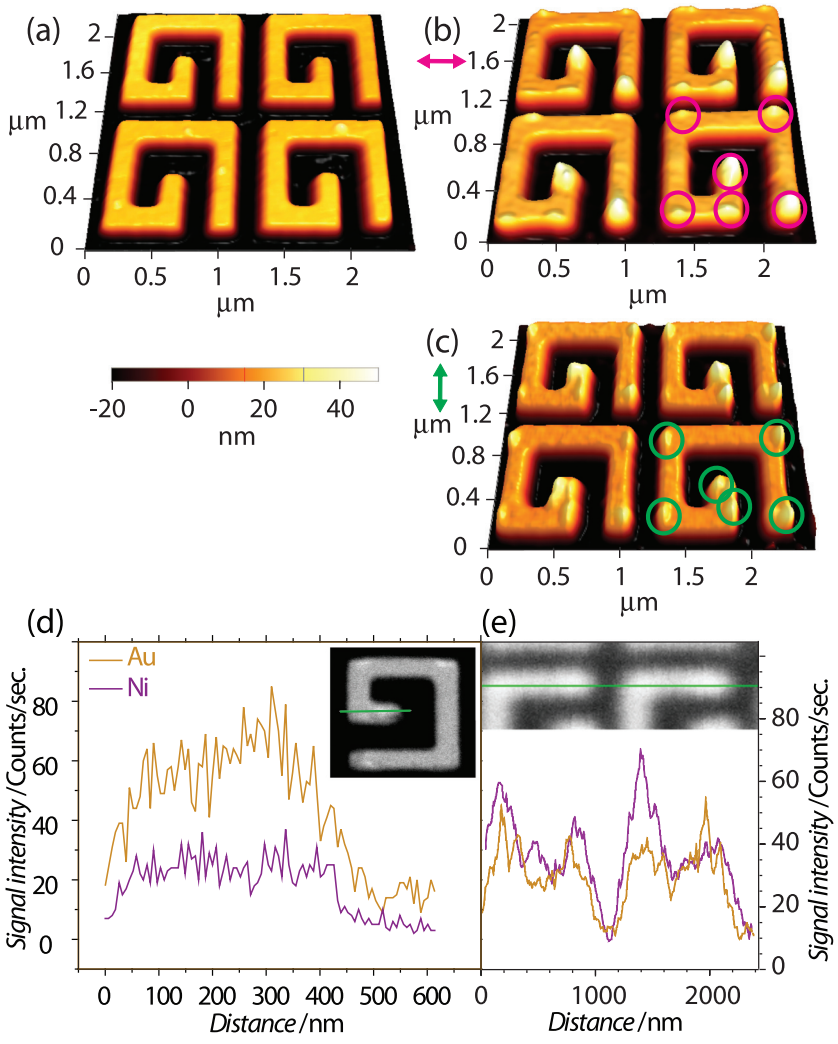


**Figure 3.** Illuminating the sample with femtosecond laser pulses produces a polarization-dependent pattern of nanobumps with sharp tips, on the sample surface. Atomic force microscopy (AFM), in (a), shows the sample before illumination. Illumination is performed with horizontally (red arrow) and vertically (green arrow) polarized light. After illumination, the AFM micrographs, in (b) and (c), demonstrate that a polarization-dependent pattern of nanobumps is present on the sample surface. For clarity, the nanobumps are highlighted by circles in red, for the horizontally polarized light, and in green, for the vertically polarized one. In (d) and (e), energy-dispersive X-ray spectroscopy scans were performed along the green lines of both insets. The results show that, on the nanobumps, sometimes the signal from gold increases while that from nickel remains the same, as shown in (d); sometimes it is the other way around and sometimes there is an increase of both the gold and nickel signal, as shown in (e). The seemingly random material content suggests that the nanobumps are most likely made of a gold/nickel melt.

occur on the vertical edges of the star. The occurrence of these hotspots is experimentally verified by means of second harmonic generation microscopy, see Figure 5c. For increasing laser power, Figure 5d and Figure 5e show that first two nanobumps appear on the hotspots and then the vertical edges melt and retract under the forces of surface tension. As can be seen in Figure 2f, these edges are 200 nm long, i.e. the length of removed material is significantly below the 800 nm wavelength of the light source. A similar process is observed for the vertical polarization, whereby the hotspots are situated on the horizontal edges of the star, see Figure 5f to Figure 5j. The figure clearly demonstrates that the temperature distribution is strongly polarization-dependent in the nanostructure. But how does this process compare with ablation levels in the absence of plasmons?

In gold film, the ablation threshold is situated within the laser fluence range of 0.4 to 1.4 J/cm$^2$ for 100 fs pulses.[24,7] It has been reported that in nanostructures, local field effects that are due to geometric features can lower the ablation threshold to 9 mJ/cm$^2$.[12] In our nanostructures, plasmonic effects can lower the threshold even further: the ablation process starts at laser fluence of 2.7 mJ/cm$^2$ and complete melting is reached for a laser fluence of 6.5 mJ/cm$^2$.

Note that in all our laser ablation experiments described above, we typically used ~45 pulses per pixel. In previous reports, however, nanojet structures have been generated on a gold film surface by tightly-focused *single* femtosecond (fs) laser pulses.[5–7] To properly compare the plasmon-assisted nanojet generation process with these previously-reported results we irradiated our nanostructures by single 30 fs laser pulses. For this purpose, a laser beam with a squared shape of 6 × 6 µm$^2$ size and flat-top intensity distribution was used (see Refs. 5 and 10 for details of the image transfer approach applied for beam shaping). The flat-top intensity distribution allowed irradiation of multiple nanostructures by a single laser pulse and at the same irradiation conditions.

**Figure 6**a shows an SEM micrograph of a G-shaped nanostructure, after illumination with horizontally polarized light. This configuration is similar to that of Figure 4c, where two very strong hotspots (in red) can be seen at the edges of the nanostructure. These hotspots can be seen, in Figure 6a, as nanobumps generated by a single 30 fs laser pulse. Upon increasing the laser power, Figure 6a to Figure 6f, the nanobumps become larger and, at laser fluence ~60 mJ/cm$^2$, they transform into nanojets. It is also apparent in Figure 6e that the nanobumps are hollow. These nanostructures are similar but significantly smaller than those generated by tightly focused single 30 fs laser pulses on a homogeneous gold film surface. Their shape can be explained by a fast local melting of a gold film, rapid hydrodynamic processes of nanojet generation and fast solidification of the nanostructures. The small size of the plasmon-generated nanojet structures opens new possibilities for molecular dynamic simulations of the nanojet formation process at experimental scales. This direct comparison of simulation results with experiments was previously not possible due to the significantly larger size of laser-generated nanojet structures.[4] At slightly higher laser fluences (83 mJ/cm$^2$,

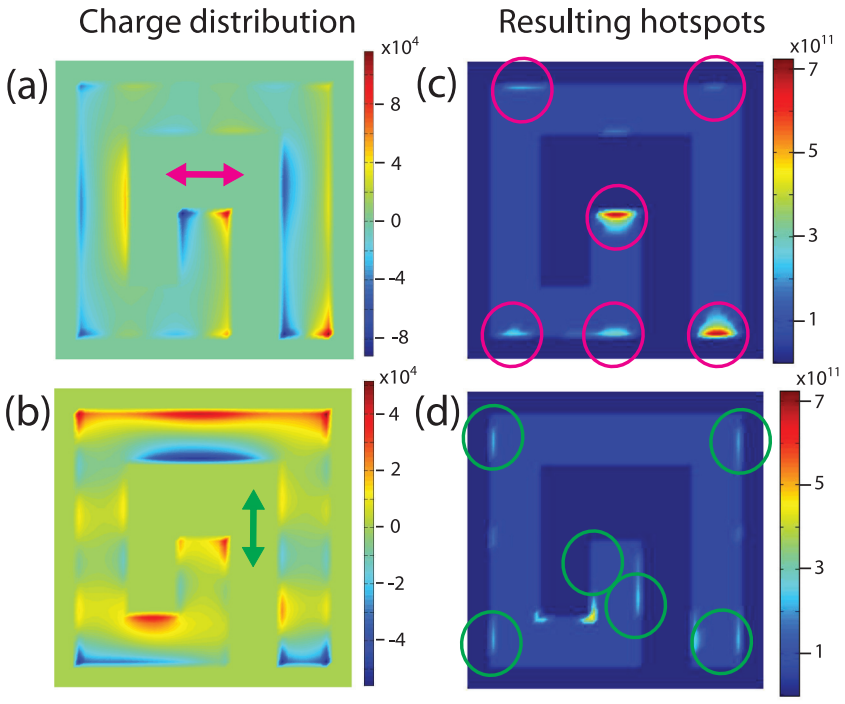


**Figure 4.** The pattern of melted nanobumps matches that of the plasmonic currents, where Ohmic losses locally increase the temperature. The electric field of light incident on the nanostructures causes the surface charges to oscillate in response to the direction of light polarization: horizontal, in (a), and vertical, in (b). The locations of the resulting electric currents, squared, are shown in (c) and (d) respectively. According to Joule's law, the squared electric current is proportional to the heating. Colored circles indicating the nanobumps are superimposed on the figures. These circles match well the pattern of hottest regions on the surface.

Figure 6f) a spherical droplet of ~40 nm radius is ejected from each hotspot, see Figure 6g. This process can further be applied to fabrication of regular structures consisting of gold nanoparticles.[7–10] The ejection of the nanodroplet leaves a metal cone on the surface of the nanostructure. The radius of curvature at the tip of the metal cones is less than 6 nm, this measurement being limited by the SEM resolution.

The results presented here are focuses on spatial control of the hotspots. It should be noted that further control could be achieved through coherent control, especially by making use of phase pulse shaping techniques.[25–30]

To summarize, we have reported that when incident upon a nanopatterned gold surface, femtosecond laser pulses can melt the material precisely in the regions of plasmonic hotspots. At the beginning of the melting process, nanobumps are observed on the surface of the nanostructure. The nanobumps often present a sharp tip, which cannot be explained by forces trying to minimize surface tension in the melted region. These nanobumps are the cooled remains of nanojets generated by the impact of femtosecond pulses on the hotspots. For increased laser power, the entire nanostructures melt starting from the plasmonic hotspots. At this stage the melting processes become dominated by forces trying to minimize the surface tension. We have also shown that upon excitation of different plasmons, depending on the polarization of light, it is possible to choose the position of the nanojets on the sample surface. For smaller nanostructures, exciting different plasmonic modes should bring further control over the position of the nanojets. At a threshold value of laser fluence of ~83 mJ/cm$^2$, the nanojets can eject very regular metal nanosphere droplets, whose radius is tuned by the geometry of the nanostructures and their plasmonic properties. These droplets can be further collected on

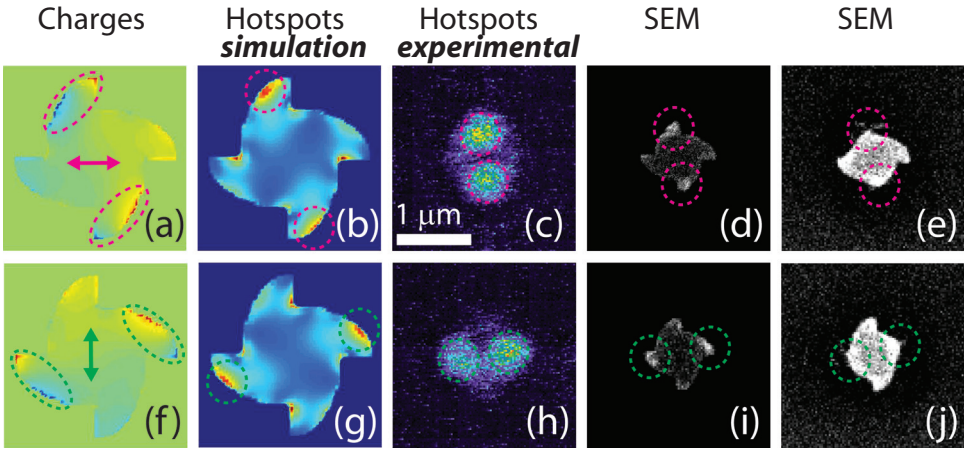


**Figure 5.** Strongly polarization-dependent heating of nanostructures by femtosecond laser pulses, due to plasmonic hotspots. For horizontally polarized light, a numerical simulation indicating the charge distribution at the surface of the nanostructure is shown in (a). The resulting electric currents are shown in (b). The hotspots were experimentally observed by means of second harmonic generation microscopy, shown in (c). In (d) and (e), Scanning electron microscopy (SEM) images of the nanostructures for laser illumination at 1 mW and 1.8 mW of laser power, respectively, are shown. On the second row, for vertically polarized light, figures (f) to (j) are organized in a similar manner.

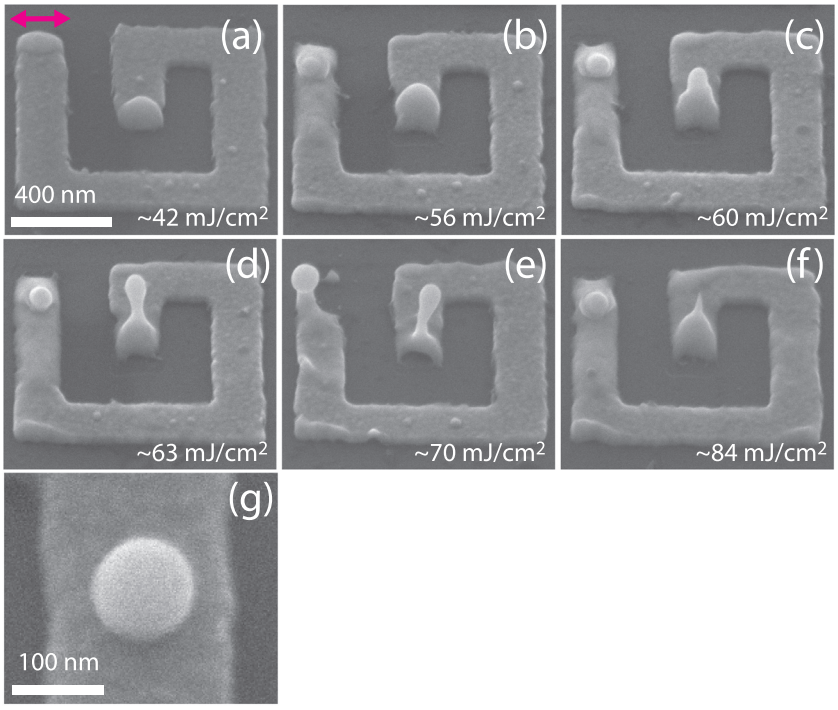


**Figure 6.** Single femtosecond pulses produce nanojets from the plasmonic hotspots. From (a) to (f), scanning electron microscopy of the G-shaped nanostructures reveals that with increasing laser power a nanobump forms, grows and results in the formation of a nanojet that ejects a nanosphere of metal. In (g) a very regular nanosphere, which has landed on the arm of a neighboring nanostructure, is shown. In (e) it is apparent that the nanobumps are hollow. The direction of light polarization is indicated with the red arrow.

a receiver substrate and assembled into regular nanoparticle structures. This method can also be applied to fabrication of electronic chips, which can be designed by first producing a matrix of disconnected transistors, and subsequently creating interconnects by laser-induced and plasmon-assisted melting.

## Experimental Section

For the preparation of the star-shaped samples, a silicon substrate covered with a thermally grown layer of silicon dioxide approximately 100 nm thick was coated with a solution of poly(methyl methacrylate) (PMMA) dissolved in anisole. The substrate was then spun at 2000 RPM for 45 seconds and then heated on a hotplate at 150 Celsius for 75 seconds producing a 100 nm thick layer of PMMA resist. The PMMA layer was then patterned using electron beam lithography (EBL) and the exposed areas of PMMA resist removed using a developer consisting of 1 part 4-Methyl-2-pentanone (MIBK) to 3 parts Isopropyl alcohol (IPA). The EBL-masked sample was then placed in a thermal evaporation chamber which was evacuated to a base pressure below $1 \times 10^{-6}$ mBar. A 5 nm chromium adhesion layer was evaporated onto the sample using a resistively heated tungsten wire basket, followed by a 35 nm gold layer deposited from a resistively heated molybdenum boat. The coated sample was then placed in an acetone bath for several hours. Sonication of the bath then removed the unexposed PMMA and its metallic coating leaving behind the metal features.

The EDS and SEM measurements in Figure 2 and Figure 4b were performed on Quantax X-ray microanalyzer, Bruker, attached to a combined instrument SEM/FIB (scanning electron microscope/focused ion beam). The EDS spectra and maps were taken at relatively low electron energy (10 kV) to minimize the substrate signal.

For the EDS and SEM measurements in Figure 4a, carbon was evaporated on the sample surface to provide a conducting layer for further examination. A high resolution scanning electron microscope (Philips XL-30 FEG) equipped with an energy dispersive spectroscopy detector system with an ultra thin window was used for qualitative determination of the composition of the different phases. Back-scattered electron (BSE) and Secondary Electron (SE) images were acquired with the help of the same device.

## Acknowledgements

We acknowledge financial support from the Research Council of KU Leuven (CREA), the fund for scientific research Flanders (FWO-V), the KU Leuven (GOA), Methusalem Funding by the Flemish government, the Belgian Inter-University Attraction Poles IAP Programmes, the DFG priority program SPP1391 "Ultrafast Nanooptics" and the Centre for Quantum Engineering and Space-Time Research (QUEST). V.K.V. and A.V.S. are grateful for the support from the FWO-Vlaanderen. O.A.A. is partly supported by the Russian Foundation for Basic Research. G.T. and S.R. are supported by the NSB of Bulgaria, grant No. DO 02-56/2008. B. DC. is thankful to the IWT.

Received: October 4, 2011
Revised: November 24, 2011
Published online: January 9, 2012

[1] D. S. Ivanov, L. V. Zhigilei, *Phys. Rev. B* **2003**, *68*, 064114.
[2] D. S. Ivanov, B. Rethfeld, G. M. O'Connor, T. J. Glynn, A. N. Volkov, L. V. Zhigilei, *Appl. Phys. A* **2008**, *92*, 791–796.
[3] Y. Nakata, T. Okada, M. Maeda, *Jpn. J. Appl. Phys.* **2003**, *42*, L1452–L1454.
[4] F. Korte, J. Koch, B. N. Chichkov, *Appl. Phys. A* **2004**, *79*, 879–88.
[5] A. I. Kuznetsov, J. Koch, B. N. Chichkov, *Appl. Phys. A* **2009**, *94*, 221–230.
[6] D. S. Ivanov, Z. Lin, B. Rethfeld, G. M. O'Connor, T. J. Glynn, L. V. Zhigilei, *J. Appl. Phys.* **2010**, *107*, 013519.
[7] A. I. Kuznetsov, J. Koch, B. N. Chichkov, *Opt. Express* **2009**, *17*, 18820–18825.
[8] A. I. Kuznetsov, A. B. Evlyukhin, C. Reinhardt, A. Seidel, R. Kiyan, W. Cheng, A. Ovsianikov, B. N. Chichkov, *J. Opt. Soc. Am. B* **2009**, *26*, B130–B138.
[9] A. I. Kuznetsov, R. Kiyan, B. N. Chichkov, *Opt. Express* **2010**, *18*, 21198–21203.
[10] A. I. Kuznetsov, A. B. Evlyukhin, M. R. Gonçalves, C. Reinhardt, A. Koroleva, M. L. Arnedillo, R. Kiyan, O. Marti, B. N. Chichkov, *ACS Nano* **2011**, *5*, 4843–4849.
[11] A. Chimmalgi, T. Y. Choi, C. P. Grigoropoulos, K. Komvopoulos, *Appl. Phys. Lett.* **2003**, *82*, 1146.
[12] S. M. Huang, M. H. Hong, Y. F. Lu, B. S. Lukyanchuk, W. D. Song, T. C. Chong, *J. Appl. Phys.* **2002**, *91*, 3268.
[13] Y. Lu, S. C. Chen, *Nanotechnology* **2003**, *14*, 505.
[14] A. Habenicht, M. Olapinski, F. Burmeister, P. Leiderer, J. Boneberg, *Science* **2005**, *309*, 2043.
[15] A. Plech, V. Kotaidis, M. Lorenc, J. Boneberg, *Nat. Phys.* **2006**, *2*, 44.

[16] S. A. Maier, *Plasmonics: Fundamentals and Applications*, Springer, New York **2007**.
[17] V. K. Valev, A. V. Silhanek, Y. Jeyaram, D. Denkova, B. De Clercq, V. Petkov, X. Zheng, V. Volskiy, W. Gillijns, G. A. E. Vandenbosch, O. A. Aktsipetrov, M. Ameloot, V. V. Moshchalkov, T. Verbiest, *Phys. Rev. Lett.* **2011**, *106*, 226803.
[18] V. K. Valev, N. Smisdom, A. V. Silhanek, B. De Clercq, W. Gillijns, M. Ameloot, V. V. Moshchalkov, T. Verbiest, *Nano Lett.* **2009**, *9*, 3945.
[19] V. K. Valev, A. V. Silhanek, N. Smisdom, B. De Clercq, W. Gillijns, O. A. Aktsipetrov, M. Ameloot, V. V. Moshchalkov, T. Verbiest, *Opt. Express* **2010**, *18*, 8286–8293.
[20] V. K. Valev, A. V. Silhanek, N. Verellen, W. Gillijns, P. Van Dorpe, G. A. E. Vandenbosch, O. A. Aktsipetrov, V. V. Moshchalkov, T. Verbiest, *Phys. Rev. Lett.* **2010**, *104*, 127401.
[21] V. K. Valev, A. Volodin, A. V. Silhanek, W. Gillijns, B. De Clercq, Y. Jeyaram, H. Paddubrouskaya, C. G. Biris, N. C. Panoiu, O. A. Aktsipetrov, M. Ameloot, V. V. Moshchalkov, T. Verbiest, *ACS Nano* **2011**, *5*, 91.
[22] V. K. Valev, X. Zheng, C. G. Biris, A. V. Silhanek, V. Volskiy, B. De Clercq, O. A. Aktsipetrov, M. Ameloot, N. C. Panoiu, G. A. E. Vandenbosch, V. V. Moshchalkov, *Opt. Mater. Express* **2011**, *1*, 36.
[23] G. A. E. Vandenbosch, V. Volski, N. Verellen, V. V. Moshchalkov, *Radio science* **2011**, *46*, RS0E02.
[24] B. C. Stuart, M. D. Feit, S. Herman, A. M. Rubenchik, B. W. Shore, M. D. Perry, *Opt. Soc. Am. B* **1996**, *13*, 459–468.
[25] M. I. Stockman, S. V. Faleev, D. J. Bergman, *Phys. Rev. Lett.* **2002**, *88*, 067402.
[26] M. I. Stockman, D. J. Bergman, T. Kobayashi, *Phys. Rev. B* **2004**, *69*, 054202.
[27] T. Brixner, F. J. García de Abajo, J. Schneider, W. Pfeiffer, *Phys. Rev. Lett.* **2005**, *95*, 093901.
[28] M. I. Stockman, P. Hewageegana, *Nano Lett.* **2005**, *5*, 2325.
[29] M. Aeschlimann, M. Bauer, D. Bayer, T. Brixner, F. J. G. d. Abajo, W. Pfeiffer, M. Rohmer, C. Spindler, F. Steeb, *Nature* **2007**, *446*, 301.
[30] M. I. Stockman, M. F. Kling, U. Kleineberg, F. Krausz, *Nat. Photon.* **2007**, *1*, 539.